Pediatrics and Neonatology (2016) 57, 318–325

Available online at www.sciencedirect.com

ScienceDirect

journal homepage: http://www.pediatr-neonatol.com

ORIGINAL ARTICLE

Microstructural Changes in Absence Seizure Children: A Diffusion Tensor Magnetic Resonance Imaging Study

Jao-Shwann Liang [a], Shiou-Ping Lee [b], Benjamin Pulli [c], John W. Chen [c], Sheng-Chuan Kao [c], Yuk-Ming Tsang [c], Kevin Li-Chun Hsieh [d,e,*]

[a] *Department of Pediatrics, Far Eastern Memorial Hospital, New Taipei City, Taiwan*
[b] *Division of Medical Imaging, Radiology Department, Far Eastern Memorial Hospital, New Taipei City, Taiwan*
[c] *Center for Systems Biology and Department of Radiology, Massachusetts General Hospital, Harvard Medical School, MA, USA*
[d] *Department of Medical Imaging, Taipei Medical University Hospital, Taipei, Taiwan*
[e] *Translational Imaging Research Center, College of Medicine, Taipei Medical University, Taipei, Taiwan*

Received Jul 21, 2015; received in revised form Sep 22, 2015; accepted Oct 13, 2015
Available online 2 December 2015

Key Words
absence seizures;
diffusion tensor imaging;
magnetic resonance imaging;
mean diffusivity;
tractography

Background: Absence seizures are a subtype of epileptic seizures clinically characterized by transient alterations in states of consciousness and by electroencephalography indicating diffuse spike-wave discharges (SWD). Conventional brain magnetic resonance imaging (MRI) is not routinely used to establish the diagnosis, but rather to rule out other diseases. The present study investigated tissue integrity in children with SWD epilepsy using diffusion tensor imaging (DTI).

Methods: Magnetic resonance imaging (MRI)-DTI was conducted in 18 patients with absence seizures and 10 control participants. Brain areas were evaluated using diffusion maps, and fractional anisotropy (FA), mean diffusivity (MD), parallel diffusivity ($\lambda\|$), and perpendicular diffusivity ($\lambda\perp$) values were extracted and analyzed. Tractography at the regions of abnormal diffusion indices was then reconstructed in each group, and tract symmetry was evaluated by an index of asymmetry (AI). Statistical analyses were performed using nonparametric Mann–Whitney *U* tests, with p values < 0.05 indicating statistical significance.

Results: Compared to the control group, patients with SWD epilepsy had lower FA values and higher MD values at the genu of the corpus callosum. There was also a stronger negative correlation between MD and FA values at the genu of the corpus callosum in patients than in

* Corresponding author. Department of Medical Imaging, Taipei Medical University Hospital, Number 252, Wu Hsing Street, Taipei City 110, Taiwan.
E-mail address: Kevinh9396@gmail.com (K.L.-C. Hsieh).

http://dx.doi.org/10.1016/j.pedneo.2015.10.003

control participants. The AI for the fiber tracts through the genu of the corpus callosum in the SWD group was significantly higher than that of the control group, indicating that tract distribution was more asymmetric in patients with epilepsy. There were no significant differences between groups in diffusion indices for other brain areas.
Conclusion: We observed microstructural changes in the genu of the corpus callosum, as well as reduced FA values, increased $\lambda\perp$ values, increased MD values, and asymmetric distribution of fiber tracts, indicating that DTI is more sensitive than conventional MRI to detect brain abnormalities in children with absence seizures.

1. Introduction

Absence epilepsy (AE) is a specific type of brief, generalized nonconvulsive epileptic seizure disorder. The seizures are characterized by a transitory alteration in consciousness associated with electroencephalograms (EEGs) indicating bilateral 3—4 Hz spike-wave discharges (SWD) of variable duration.[1] There are three different types of absence seizures: childhood AE, juvenile AE, and epilepsy with myoclonic absences.[2,3] Although the prognosis is usually favorable in AE, cognitive changes as well as linguistic and behavioral problems may occur. In addition, improvements in cognition are observed only after patients are seizure-free and EEG no longer shows any SW complexes.[2]

Typical SWD in absence seizures is dependent on long-range corticothalamic and corticocortical network interactions.[1,4,5] In addition, the largest SWD amplitude typically occurs in the midline frontal region near the central sulcus, and in the occipital regions.[6—8] However, results from conventional magnetic resonance imaging (MRI) studies have not demonstrated specific pathology.[9] Advanced MRI sequences may provide more specific diagnostic information for use in investigating microstructural abnormalities in patients with AE.

Diffusion tensor imaging (DTI) noninvasively maps white matter tracts in the human brain.[10,11] DTI data is described by an anisotropic diffusion displacement-probability ellipsoid, characterized by three eigenvalues ($\lambda1$, $\lambda2$, and $\lambda3$) and three eigenvectors (e1, e2, and e3) in a local frame of each image voxel after matrix diagonalization. The average of the three eigenvalues is referred to as the mean diffusivity (MD), which is a directionally averaged measure of water diffusion that reflects tissue density. Fractional anisotropy (FA) quantifies the degree of preferred directionality for water displacement, and is a marker for diffusion anisotropy. These indices allow quantitative evaluation of the magnitude and degree of anisotropy for the random translational motion of water molecules. Both FA and MD are sensitive to a variety of brain pathologies affecting white matter integrity, including epilepsy.[12,13]

Although epilepsy is generally not considered a white matter disease, it occurs with increased incidence in patients with multiple sclerosis,[14] and can be associated with abnormal myelination.[15] Data from previous DTI studies have demonstrated abnormal diffusion indices in prefrontal areas of seizure patients,[13] including cortical malformation-related epilepsy and unilateral temporal lobe epilepsy.[16] In addition, Chahboune et al[17] found abnormal diffusion indices at the anterior corpus callosum in a rat model of absence seizure, suggesting that chronic SWD in the cortex may result in microstructural changes in white matter pathways.[17] However, generalized seizures involving the WAG/Rij rat may or may not be equivalent to human absence seizures.[2] Therefore, the present study investigated white matter integrity using DTI-derived FA, MD, and tractography in children with absence seizures and diffuse SWD, compared to control participants.

2. Methods

2.1. Patient selection

This prospective case—control study was approved by the Institutional Review Board of Far Eastern Memorial Hospital. Participant confidentiality and privacy were protected according to national standards. Informed consent was obtained from each participant and/or his or her parents. Eighteen right-handed patients with absence seizures and diffuse SWD were included in this study. Medical histories, neurological examinations, and routine EEG recordings were conducted for each participant, and diagnosis was then established according to the diagnostic criteria of the International League Against Epilepsy.[18] Inclusion criteria were as follows: (1) age of onset between 3 years and 18 years; (2) absence seizures as the main seizure type; (3) absence seizures associated with bilateral, synchronous, and symmetrical 3 Hz SWD with normal background; and (4) normal neurological examination. Ten patients were diagnosed with childhood absence epilepsy, five patients with juvenile AE, and three patients with drug-induced AE. The clinical data are presented in Table 1. Ten right-handed healthy participants [6 girls and 4 boys; mean age 10.6 years, standard deviation (SD) 3.8 years] with no history of neurological disorders and a normal neurological examination served as controls. When imaging yielded obviously detectable abnormalities or poor image quality, participants were excluded from the study ($n = 4$).

2.2. Image acquisition

All participants had MRIs within 6 months of diagnosis, and all exams were performed between ictal episodes and

Table 1 Demographic data of 18 patients with absence seizure.

Patient No.	Age (y), gender[§]	Seizure onset age	Seizure duration (mo) *	Seizure type, frequency	Seizure focality †	Antiepileptic medication ‡	Diagnosis
1	11, F	9 y 6 mo	30	AS, 10–20/d	Bilateral frontal	VPA	CAE
2	8, F	7 y 4 mo	25	AS, 10–20/d	Bilateral frontal	None	CAE
3	13, F	6 y 5 mo	18	AS, several/d	Bilateral centro-temporal	VPA	CAE
4	15, F	10 y	90	AS, several/d	Left frontal	VPA	CAE
5	6, F	6 y	65	AS, 2–3/d	Left frontal	None	CAE
6	9, M	7 y	61	AS, 10–20/d	Bilateral frontal	None	CAE
7	16, M	5 y	22	AS, 7–8/d	Right temporal	VPA	CAE
8	9, F	8 y 8 mo	14	AS, several/d	Bilateral frontal/temporal	None	CAE
9	13, M	8 y	48	GTC/AS, several/d	Bilateral frontal	VPA	CAE
10	9, M	8 y 5 mo	18	AS, several/d	Right central	None	CAE, FC
11	16, F	12 y 8 mo	20	GTCS/AS, several/d	Bilateral frontal	VPA	JAE
12	15, F	12 y 1 mo	9	GTCS/AS, several/d	Bilateral frontal	LTG	JAE
13	16, F	12 y	2	GTCS/AS, 6–7/d	Right centro-temporal	VPA	JAE
14	12, M	11 y 6 mo	41	GTCS/AS, several/d	Bilateral frontal & left temporal	None	JAE
15	17, M	13 y	33	GTCS/AS, several/d	Bilateral frontal	VPA	JAE, FC
16	6, M	4 y 4 mo	12	GTCS/AS, several/d	Bilateral frontal	VPA	Drug induced: OXC
17	19, F	5 y 3 mo	116	AS, several/d	Bilateral frontal	VPA	Drug induced: OXC
18	17, F	15 y	9	GTCS /AS, several/d	Bilateral frontal	VPA	Drug induced: TPM

AS = absence seizure; CAE = childhood absence epilepsy; FC = febrile convulsion; GTCS = generalized tonic–clonic seizure; JAE = juvenile absence epilepsy; LTG = lamotrigine; OXC = oxcarbazepine; TPM = topiramate; VPA = valproic acid.

* Length of seizure history from first seizure-onset to the date of magnetic resonance imaging (MRI) study.

† Focus of epileptiform discharges during the interictal electroencephalogram (EEG) or follow-up EEG.

‡ Antiepileptic medication use while magnetic resonance imaging (MRI) was acquired.

§ All patients are right-handed.

before any medical treatment. Specialized epilepsy sequences were obtained on a 1.5T MR scanner (Magnatom Avanto; Siemens Healthcare, Erlangen, Germany), including DTI, using parallel acquisition techniques (PAT 2 GRAPPA), single shot spin-echo diffusion echo planar imaging: repetition time (TR) = 8800 milliseconds, echo time (TE) = 98 milliseconds, two averages, field of view = 280 mm, 55 axial slices with no gap, acquisition isotropic voxel resolution of $2.2 \times 2.2 \times 2.2$ mm^3. The total scan time was 4 minutes. The diffusion tensor was acquired with diffusion gradients along six noncollinear directions (b = 1000 s/mm^2) and one direction without diffusion weighting (b = 0 s/mm^2). The six independent elements of the diffusion tensor were calculated from each series of diffusion-weighted images. The resulting tensor element maps were used to derive the eigenvalues ($\lambda1$, $\lambda2$, and $\lambda3$) and the corresponding eigenvectors (e1, e2, and e3) of the diffusion tensor by matrix diagonalization.[19,20] Maps of FA, principal eigenvalues ($\lambda1$, $\lambda2$, and $\lambda3$) and MD (the mean of the 3 principal eigenvalues) were then calculated for each slice using custom software developed in our lab. The parallel diffusivity ($\lambda||$) value was derived from the largest eigenvalues ($\lambda|| = \lambda1$), while perpendicular diffusivity ($\lambda\perp$) was derived from the mean of two smaller eigenvalues ($\ddot{e}\perp = (\lambda2 + \lambda3)/2$) on a pixel-by-pixel basis. Three dimensional T1-weighted image (TR = 2000 milliseconds, TE = 2.96 milliseconds), and T2 fluid-attenuated inversion recovery (FLAIR) image (TR = 9000 milliseconds, TE = 85 milliseconds) were also acquired.

2.3. Image analyses and post-processing

Two observers (S.P.L. and K.H.) blinded to patient identity reviewed the entire image sets to look for gross anomalies, including abnormal T1 or T2 signals and pathological structures such as tumor or congenital malformations. Participants whose images had obviously detectable abnormalities or poor image quality were excluded from the study. Regions-of-interest (ROIs) were drawn manually within visible hyperintensities on the nondiffusion weighted (i.e., b = 0 s/mm^2) images and transferred to the diffusion parametric maps for each participant, by the same observers. The anterior frontal white matter, posterior frontal white matter, temporal white matter, genu of the corpus callosum, anterior limb of the internal capsule, and posterior limbs of the internal capsule were identified on axial sections at the level of the lateral ventricles. The body of the corpus callosum was identified at the mid-sagittal plane between the two lateral ventricles, which can be easily recognized by its strong FA signal. The ROI size in each

anatomical region was the same for all participants. FA, MD, λ||, and λ⊥ were measured within the selected ROIs.

2.4. Fiber tractography

The tensor deflection tractography method was applied to capture propagative vectors with adaptive stepping size, because it can track fiber bundles in curved and crossing fibers, beyond diffusion tensor limitations.[21] Propagation in each fiber tract was terminated if a voxel with an FA value < 0.15 was reached, or if the inner product of two consecutive vectors was > 0.7. Tracking results that penetrated the manually segmented ROIs at the genu of the corpus callosum were assigned to specific tracts. ROI manipulations were performed by one blinded neuroradiologist (K.H.) with 6 years of experience performing tractography and 7 years of experience as a neuroradiologist. All software used for reconstruction of the tractography fibers was developed using MATLAB (version 7.0.4, 2005, The MathWorks, Natick, MA, USA).

2.5. Evaluation of tractography

In addition to counting the total number of tracts obtained from the reconstruction, the index of asymmetry (AI) between the right (R) and left (L) side tracts was calculated for each participant. Values were obtained by calculating the absolute difference in number of fibers between the two sides, divided by the mean of the two sides, as modified from a previously described method:[22]

$$AI = L - R/[(L + R)/2]. \quad (1)$$

AIs were calculated for both the SWD and control groups.

2.6. Statistical analyses

All data were analyzed using nonparametric Mann–Whitney *U* tests. Gender and age differences between groups were assessed with Fisher's exact test and the Student *t* test, respectively. For age, mean range and/or SD are presented. Mean and SD are presented for diffusion values. All analyses were performed using Prism (release 6.0, GraphPad Software Inc., La Jolla, CA, USA). A p value ≤ 0.05 was considered statistically significant.

3. Results

3.1. FA and MD

FA, MD, λ||, and λ⊥ were measured in seven anatomical regions. Significantly lower FA values were recorded at the genu of the corpus callosum (Figure 1) in the epilepsy group compared to the control group (0.61 ± 0.12 vs. 0.65 ± 0.01; $p = 0.03$). Significantly higher MD values (0.78 ± 0.04 vs. 0.71 ± 0.01; $p = 0.03$) and λ⊥ values (0.50 ± 0.04 vs. 0.42 ± 0.03; $p = 0.01$) were also observed in the genu of the corpus callosum.

In the other anatomical regions, including the anterior and posterior frontal white matter, anterior and posterior limbs of the internal capsules, temporal white matter, and body of corpus callosum, no significant differences were observed (Figure 2).

In addition, we found a significant negative correlation between MD and FA at the genu of the corpus callosum in the epilepsy group ($r = -0.83$, $p < 0.001$), but not in the control group ($r = -0.14$, $p = 0.68$, Figure 3).

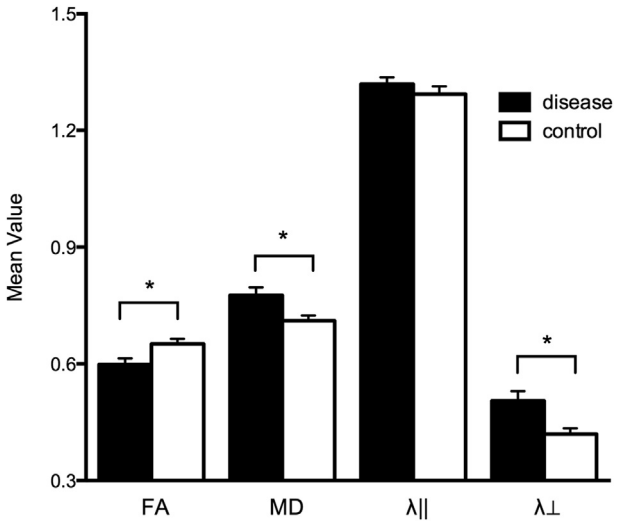

Figure 1 Diffusion parameter in the genu of the corpus callosum, comparing spike-wave epilepsy and control groups. Four diffusion parameter values are shown for each of the two groups. Mean diffusivity (MD) and radial diffusivity (λ⊥) are higher, and fractional anisotropy (FA) values lower, in the spike-wave discharge (SWD) group than in the control group (*). λ|| = axial diffusivity; λ⊥ = radial diffusivity; FA = fractional anisotropy; MD = mean diffusivity.

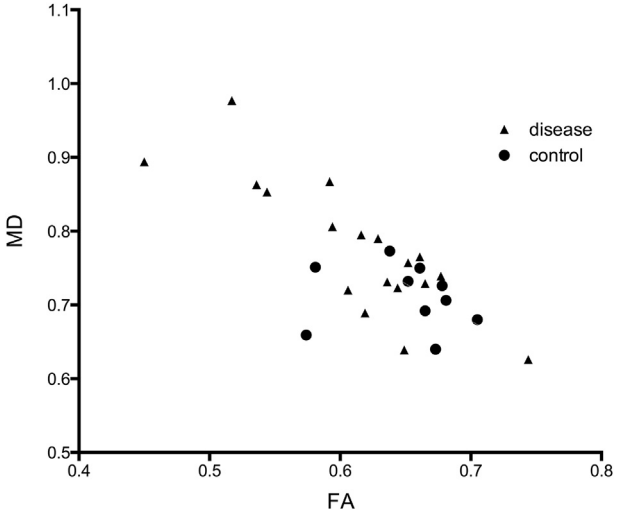

Figure 2 Correlation between fractional anisotropy (FA) and mean diffusivity (MD) values in patients with spike-wave epilepsy and control participants. Strong negative correlations occurred between FA and MD, particularly in the spike-wave discharge (SWD) group (▲). FA = fractional anisotropy; MD = mean diffusivity.

3.2. DTI tractography at the anterior corpus callosum

We used tractography to determine the anatomical course of the white matter pathways passing through the genu of corpus callosum (Figure 4), which showed that these fibers interconnect the bilateral frontal cortices, as predicted.

Comparisons of the shape symmetry of bilateral tracts through the genu ROI revealed that nearly all tracts had asymmetric geographic distribution in both groups. The results for absolute tract numbers revealed that nine patients with SWD epilepsy were dominant on the right side and 11 patients were dominant on the left side. In the control group, four participants were dominant on the right side and six participants were dominant on the left side. Although there was no significant difference in the total tract number between the two groups (Figure 4, $p = 0.19$), the mean AI in the SWD group was significantly higher compared to the control group (0.42 ± 0.09 vs. 0.19 ± 0.05, $p = 0.02$, Figure 5C). These results demonstrate that the tract distribution through the genu was more asymmetric in the SWD group compared to the control group (Figures 5A and 5B).

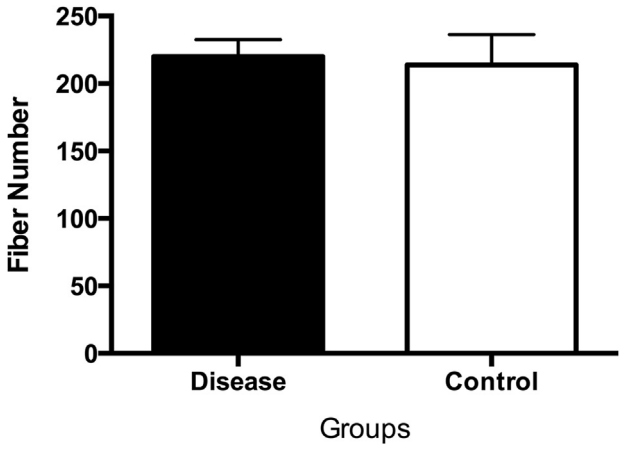

Figure 4 Total number of tracts through the genu of the corpus callosum. No significant difference is observed ($p = 0.19$).

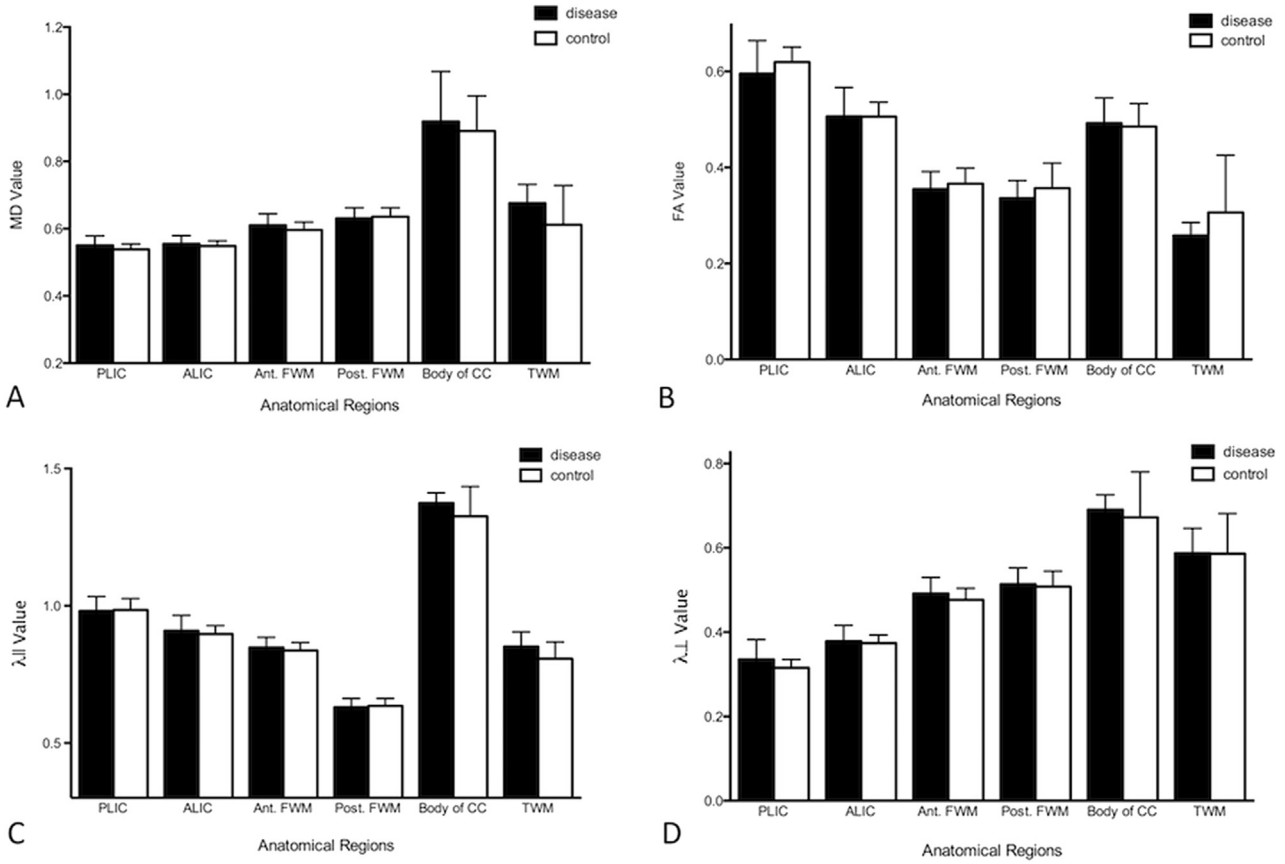

Figure 3 Diffusion index values in anatomical brain regions. There is no significant difference between the patient and control groups for: (A) mean diffusivity (MD); (B) fractional anisotropy (FA); (C) axial diffusivity (λ||); or (D) radial diffusivity (λ⊥). ALIC = anterior limb of the internal capsule; Ant. FWM = anterior frontal white matter; Body of CC = body of corpus callosum; MD = mean diffusivity; PLIC = posterior limb of the internal capsule; Post. FWM = posterior frontal white matter; TWM = temporal lobe white matter.

We also investigated a correlation between the length of seizure history (seizure duration) and FA, MD, $\lambda\perp$, and AI values for the corpus callosum, in order to assess whether white matter declines are related to disease duration. However, no significant correlation occurred for any of the diffusion tensor parameters.

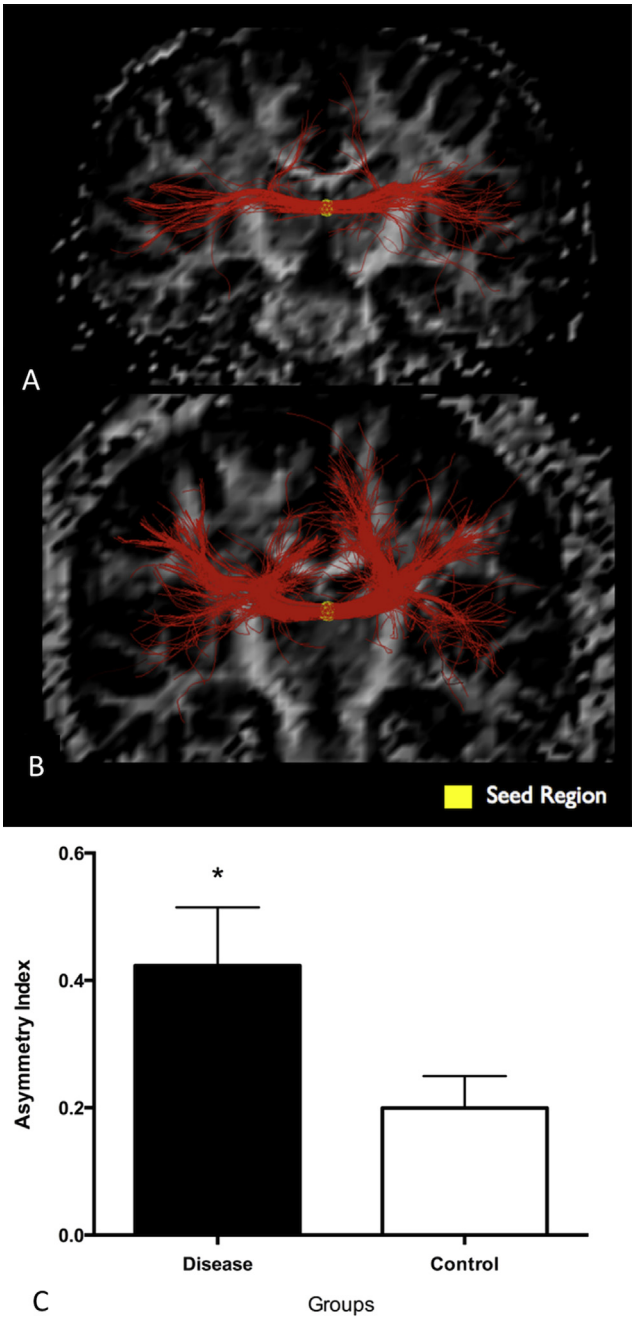

Figure 5 Comparison of asymmetry indices (AI) for the genu of the corpus callosum in (5A) control and (5B) spike-wave discharge (SWD) groups. Regions-of-interest (ROIs) for tracts through the genu of the patients with SWD are more asymmetric in distribution compared to the control participants. (5C) Significantly higher AIs are observed in the SWD group, indicating more asymmetric distribution of the tracts ($p = 0.02$).

4. Discussion

In pediatric patients with absence seizures, we found significantly lower FA and higher MD values at the genu of the corpus callosum, and also identified a significant negative correlation between MD and FA values in the genu of the corpus callosum. The reduced FA values were related to increased perpendicular diffusivity, without significant changes in parallel diffusivity. The area of the anterior corpus callosum exhibiting these changes interconnects the bilateral frontal cortices, where animal studies have shown epileptogenic discharges.[23,24] Our results in humans are consistent with a study by Chahboune et al[17] in a rat spike-wave epilepsy model. Furthermore, our patient group showed more asymmetric tract distribution at the genu of the corpus callosum compared to the control group.

Decreased FA values may result from decreased diffusivity parallel to axonal fibers, or from increased perpendicular diffusivity.[25] Electron microcopy in areas with decreased FA values and increased $\lambda\perp$ values has demonstrated a reduction in axons or myelin.[26,27] Accordingly, we also found decreased FA and increased $\lambda\perp$ in our patient group, suggesting a reduction in axons or myelin in the affected white matter. Similar results were previously observed in the fornix of patients with temporal lobe epilepsy.[26] Decreased FA values and increased MD values were observed in a mouse model of optic nerve injury, without significant axonal cytoskeletal damage,[28] and it has been hypothesized that axonal injury without demyelination may result in decreased axial diffusivity.[29] Together, our findings show that abnormal epileptic activity in the cortex during absence seizures is related to microstructural changes in white matter pathways that connect regions of seizure discharges, and may result from axonal loss with or without demyelination.

Despite the detection of a similar number of total tracts in tractographies for both groups, a comparison of AIs indicated that genu tracts were more asymmetrically distributed in the SWD group. Although the diffusion characteristics of healthy brains may be minimally asymmetric in some tracts,[30] asymmetry may also result from damage to regional connections.[31] Our findings demonstrating abnormal diffusion parameters in conjunction with increased AI suggest that there was damage in the regional (e.g., genu) connections in patients with SWD. The damage at the genu did not affect the total number of tracts, but resulted in a change to the distribution of tracts. This finding explains the similarity in the size of the corpus callosum in patients with epilepsy versus control participants reported in a previous study.[32] Furthermore, Lüders et al[33] measured interhemispheric SWD latency differences of up to 20 milliseconds, and our results demonstrating tract asymmetry in patients with absence seizures may explain this phenomenon. Together, the findings suggest that DTI may be useful for monitoring tissue repair and/or damage, as well as for therapy, although more extensive long-term follow-up studies are needed to evaluate these potential applications.

Our data indicate that DTI abnormalities in the corpus callosum are associated with absence seizures. The genu of the corpus callosum is the anterior bend of the corpus

callosum, which contains axons connecting the frontal lobes, including the prefrontal and premotor areas.[34] This is therefore an area of critical connections for interhemispheric propagation of epileptic activity, and which has previously been shown to play a role in SWD synchrony.[35,36] A large degree of transhemispheric coherence was demonstrated between the right and left somatosensory cortices during SWD in a genetic rat absence seizure model,[37] suggesting the involvement of the corpus callosum in the pathophysiology of this disease, and also supporting the hypothesis that SWD originate from the lateral frontoparietal cortical area.

Although both control and patient groups in this study have similar baseline characteristics, including age distribution, we should still keep in mind that age may confound FA and MD measurements.[38] The majority of our participants reported symptom onset in childhood; however, the corpus callosum reaches its maximal myelination in late adolescence/early adulthood,[39] which may result in some selection bias in our measurements.

Limitations of the present study include its relatively small sample size, which limits extrapolation of our results to the general population. In addition, although there is no correlation of the history of seizure length with these microstructural damages, it is still difficult to confirm whether decreased white matter integrity is a predisposing factor to seizures, or whether chronic epilepsy damages white matter.

In conclusion, we found DTI abnormalities in the anterior corpus callosum of children with SWD epilepsy in the white matter pathway interconnecting bilateral frontal cortical regions. The abnormalities suggest that microstructural pathological changes occur in the white matter and are associated with this disorder. Furthermore, these microstructural changes may contribute to neurological abnormalities in AE. Thus, DTI-derived measures may be promising MRI markers for monitoring the progression and effects of treatment in patients with absence seizures.

Conflicts of interest

None of the authors has any conflict of interest to disclose. We confirm that we have read the Journal's position on issues involved in ethical publication and affirm that this report is consistent with those guidelines.

References

1. Blumenfeld H. Cellular and network mechanisms of spike-wave seizures. *Epilepsia* 2005;**46**:21—33.
2. Hughes JR. Absence seizures: a review of recent reports with new concepts. *Epilepsy Behav* 2009;**15**:404—12.
3. Panayiotopoulos CP, Michael M, Sanders S, Valeta T, Koutroumanidis M. Benign childhood focal epilepsies: assessment of established and newly recognized syndromes. *Brain* 2008;**131**:2264—86.
4. Avoli M, Gloor P. Interaction of cortex and thalamus in spike and wave discharges of feline generalized penicillin epilepsy. *Exp Neurol* 1982;**76**:196—217.
5. Meeren H, van Luijtelaar G, Lopes da Silva F, Coenen A. Evolving concepts on the pathophysiology of absence seizures: the cortical focus theory. *Arch Neurol* 2005;**62**:371—6.
6. Weir B. The morphology of the spike-wave complex. *Electroencephalogr Clin Neurophysiol* 1965;**19**:284—90.
7. Rodin E, Ancheta O. Cerebral electrical fields during petit mal absences. *Electroencephalogr Clin Neurophysiol* 1987;**66**:457—66.
8. Holmes MD, Brown M, Tucker DM. Are "generalized" seizures truly generalized? Evidence of localized mesial frontal and frontopolar discharges in absence. *Epilepsia* 2004;**45**:1568—79.
9. Betting LE, Mory SB, Lopes-Cendes I, Li LM, Guerreiro MM, Guerreiro CA, et al. MRI reveals structural abnormalities in patients with idiopathic generalized epilepsy. *Neurology* 2006;**67**:848—52.
10. Mori S, Crain BJ, Chacko VP, van Zijl PC. Three-dimensional tracking of axonal projections in the brain by magnetic resonance imaging. *Ann Neurol* 1999;**45**:265—9.
11. Conturo TE, Lori NF, Cull TS, Akbudak E, Snyder AZ, Shimony JS, et al. Tracking neuronal fiber pathways in the living human brain. *Proc Natl Acad Sci U S A* 1999;**96**:10422—7.
12. Lee SK, Kim DI, Kim J, Kim DJ, Kim HD, Kim DS, et al. Diffusion-tensor MR imaging and fiber tractography: a new method of describing aberrant fiber connections in developmental CNS anomalies. *Radiographics* 2005;**25**:53—65. discussion 66—8.
13. Yogarajah M, Duncan JS. Diffusion-based magnetic resonance imaging and tractography in epilepsy. *Epilepsia* 2008;**49**:189—200.
14. Koch M, Uyttenboogaart M, Polman S, De Keyser J. Seizures in multiple sclerosis. *Epilepsia* 2008;**49**:948—53.
15. Muroi J, Okuno T, Kuno C, Yorifuji T, Shimizu K, Matsumura M, et al. An MRI study of the myelination pattern in West syndrome. *Brain Dev* 1996;**18**:179—84.
16. Concha L, Beaulieu C, Gross DW. Bilateral limbic diffusion abnormalities in unilateral temporal lobe epilepsy. *Ann Neurol* 2005;**57**:188—96.
17. Chahboune H, Mishra AM, DeSalvo MN, Staib LH, Purcaro M, Scheinost D, et al. DTI abnormalities in anterior corpus callosum of rats with spike-wave epilepsy. *Neuroimage* 2009;**47**:459—66.
18. Engel Jr J, International League Against Epilepsy (ILAE). A proposed diagnostic scheme for people with epileptic seizures and with epilepsy: report of the ILAE Task Force on Classification and Terminology. *Epilepsia* 2001;**42**:796—803.
19. Hasan KM, Basser PJ, Parker DL, Alexander AL. Analytical computation of the eigenvalues and eigenvectors in DT-MRI. *J Magn Reson* 2001;**152**:41—7.
20. Jones DK, Horsfield MA, Simmons A. Optimal strategies for measuring diffusion in anisotropic systems by magnetic resonance imaging. *Magn Reson Med* 1999;**42**:515—25.
21. Chou MC, Wu ML, Chen CY, Wang CY, Huang TY, Liu YJ, et al. Tensor deflection (TEND) tractography with adaptive subvoxel stepping. *J Magn Reson Imaging* 2006;**24**:451—8.
22. Glenn OA, Henry RG, Berman JI, Chang PC, Miller SP, Vigneron DB, et al. DTI-based three-dimensional tractography detects differences in the pyramidal tracts of infants and children with congenital hemiparesis. *J Magn Reson Imaging* 2003;**18**:641—8.
23. Meeren HK, Pijn JP, Van Luijtelaar EL, Coenen AM, Lopes da Silva FH. Cortical focus drives widespread corticothalamic networks during spontaneous absence seizures in rats. *J Neurosci* 2002;**22**:1480—95.
24. Nersesyan H, Hyder F, Rothman DL, Blumenfeld H. Dynamic fMRI and EEG recordings during spike-wave seizures and generalized tonic-clonic seizures in WAG/Rij rats. *J Cereb Blood Flow Metab* 2004;**24**:589—99.
25. Beaulieu C. The basis of anisotropic water diffusion in the nervous system - a technical review. *NMR Biomed* 2002;**15**:435—55.

26. Concha L, Livy DJ, Gross DW, Wheatley BM, Beaulieu C. Direct correlation between diffusion tensor imaging and electron microscopy of the fornix in humans with temporal lobe epilepsy. *Proc Intl Soc Mag Reson Med* 2008;**16**:566.
27. Harsan LA, Poulet P, Guignard B, Steibel J, Parizel N, de Sousa PL, et al. Brain dysmyelination and recovery assessment by noninvasive in vivo diffusion tensor magnetic resonance imaging. *J Neurosci Res* 2006;**83**:392—402.
28. Song SK, Sun SW, Ju WK, Lin SJ, Cross AH, Neufeld AH. Diffusion tensor imaging detects and differentiates axon and myelin degeneration in mouse optic nerve after retinal ischemia. *Neuroimage* 2003;**20**:1714—22.
29. Xu J, Sun SW, Naismith RT, Snyder AZ, Cross AH, Song SK. Assessing optic nerve pathology with diffusion MRI: from mouse to human. *NMR Biomed* 2008;**21**:928—40.
30. Zhai G, Lin W, Wilber KP, Gerig G, Gilmore JH. Comparisons of regional white matter diffusion in healthy neonates and adults performed with a 3.0-T head-only MR imaging unit. *Radiology* 2003;**229**:673—81.
31. Semenza C, Cavinato M, Rigon J, Battel I, Meneghello F, Venneri A. Persistent cortical deafness: a voxel-based morphometry and tractography study. *Neuropsychology* 2012; **26**:675—83.
32. Hutchinson E, Pulsipher D, Dabbs K, Myers y Gutierrez A, Sheth R, Jones J, et al. Children with new-onset epilepsy exhibit diffusion abnormalities in cerebral white matter in the absence of volumetric differences. *Epilepsy Res* 2012;**88**: 208—14.
33. Lüders H, Lesser RP, Dinner DS, Morris 3rd HH. Generalized epilepsies: a review. *Cleve Clin Q* 1984;**51**:205—26.
34. Hofer S, Frahm J. Topography of the human corpus callosum revisited—comprehensive fiber tractography using diffusion tensor magnetic resonance imaging. *Neuroimage* 2006;**32**: 989—94.
35. Vergnes M, Marescaux C, Depaulis A. Mapping of spontaneous spike and wave discharges in Wistar rats with genetic generalized non-convulsive epilepsy. *Brain Res* 1990;**523**:87—91.
36. Musgrave J, Gloor P. The role of the corpus callosum in bilateral interhemispheric synchrony of spike and wave discharge in feline generalized penicillin epilepsy. *Epilepsia* 1980;**21**: 369—78.
37. Sitnikova E, van Luijtelaar G. Cortical and thalamic coherence during spike-wave seizures in WAG/Rij rats. *Epilepsy Res* 2006; **71**:159—80.
38. Lebel C, Beaulieu C. Longitudinal development of human brain wiring continues from childhood into adulthood. *J Neurosci* 2011;**31**:10937—47.
39. Keshavan MS, Diwadkar VA, DeBellis M, Dick E, Kotwal R, Rosenberg DR, et al. Development of the corpus callosum in childhood, adolescence and early adulthood. *Life Sci* 2002;**70**: 1909—22.